

## Experimental study of fluid flow in the entrance of a sinusoidal channel

F. Oviedo-Tolentino<sup>a</sup>, R. Romero-Méndez<sup>b,1</sup>, A. Hernández-Guerrero<sup>a,\*</sup>, B. Girón-Palomares<sup>a</sup>

<sup>a</sup> Facultad de Ingeniería Mecánica, Universidad de Guanajuato, Tampico 912, Salamanca, Guanajuato 36730, Mexico

<sup>b</sup> Facultad de Ingeniería, Universidad Autónoma de San Luis Potosí, Av. Dr. Manuel Nava 8, Zona Universitaria, San Luis Potosí, SLP 78290, Mexico

### ARTICLE INFO

#### Article history:

Received 2 November 2007

Received in revised form 16 January 2008

Accepted 10 March 2008

Available online 22 May 2008

#### Keywords:

Sinusoidal channel

Phase angle

Unsteady flow

Steady flow

Recirculation

Significant mixing

### ABSTRACT

An experimental flow visualization study of the entrance section of channels formed with sinusoidal plates was made. The experiments were conducted in a water tunnel and a laser illuminated particle tracking was used as the technique of flow visualization. The geometric parameters of the plates were maintained constant while the distance between plates, phase angle, and the Reynolds number were varied during the experiments. The flow regimes that were found in the experiments are steady, unsteady and significantly-mixed flows. Instabilities of the flow first appear near the exit of the channel, and move closer to the inlet waves as the Reynolds number grows, but in the first wave from inlet the flow is always steady. The results show that, for all other parameters fixed, the Reynolds number at which unsteady flow first appears grows with the distance between plates. The phase angle that best promotes unsteady flow depends on the average distance between plates: for certain average distance between plates, there is a phase angle that best disturbs the flow. For the set of parameters used in this experiment, a channel with eight waves is sufficiently long and the flow features presented in the first eight waves of a longer channel will be similar to what was observed here.

© 2008 Elsevier Inc. All rights reserved.

## 1. Introduction

Corrugated channels are used in a great variety of heat transfer situations. The corrugations in the plates forming the channel have the function of stimulating mixing of fluid within the channel. Mixing reduces variations in the temperature of the working fluid, steeping the temperature gradient near the boundaries and increasing the heat transfer between fluid and channel walls. In many applications, because of the small distance between plates or the viscosity of the working fluid, the flow in this kind of channels may occur at low Reynolds numbers. Therefore, it is advantageous to develop laminar flows with good mixing characteristics for wavy channels.

There are several geometries that have been devised to generate flow mixing within channels formed by a pair of parallel plates. An interesting option is to make the fluid to flow within a channel formed by a pair of wavy plates. The wavy channels have the characteristic of disturbing, at relatively low Reynolds numbers, the current of fluid that crosses them. A number of researchers have performed studies related to the subject, for example Asako and Faghri (1987), showed that the heat transfer of a channel formed by sinusoidal corrugated plates could be 40% larger than the heat transfer of a flat plates channel with similar Reynolds number,

pressure drop, pumping power or mass flow. Gschwind et al. (1995), made a study of mass transfer in channels with sinusoidal waves in phase. They made variations of the Reynolds number and the average distance between plates. Their results showed a large variation of the local heat and mass transfer coefficients. When varying the distance between plates and the Reynolds number, instabilities appeared, especially for small values of separation between plates. Wang et al. (1999) conducted studies aimed at finding a correlation for tube heat exchangers finned with wavy plates. Their study considered the effect of the variation of some of the heat exchanger geometric parameters. Tsal et al. (1999) carried out the numerical simulation of flow in the passages formed in the air side of a wavy finned tubes heat exchanger. Their modeling intended to determine the parameters responsible for the increase in heat transfer in wavy fins, and to take them into account to improve the design of the devices. An analytical study of a Stokes flow in a wavy channel was made by Vasudeviah and Balamurugan (2001). They demonstrated that for those conditions of flow, the contractions offer resistance to fluid flow, and a viscous heat generation exists consequently. Additionally, they concluded that for Stokes flows the rate of heat transfer of a wavy walled channel is inferior to the one of a flat walled channel. Wang and Chen (2002) used a transformation method to study the heat transfer for flows inside convergent and divergent sinusoidal channels. In that study they varied the Reynolds number and geometry. They showed that wavy channels are an effective way to increase heat transfer when the ratio amplitude to wavelength is high, and

\* Corresponding author. Tel./fax: +52 464 64 79940.

E-mail address: [abelh@salamanca.ugto.mx](mailto:abelh@salamanca.ugto.mx) (A. Hernández-Guerrero).

<sup>1</sup> Tel.: +52 444 81 73381.

## Nomenclature

$h$	average channel width $h = \frac{H_{\min} + H_{\max}}{2}$
$H_{\max}$	maximum distance between plates
$H_{\min}$	minimum distance between plates
$V$	average fluid velocity
$A$	wave amplitude of sinusoidal plates

$Re$	Reynolds number based on average distance between plates $Re = Vh/\nu$
$\nu$	kinematic viscosity
$\beta$	phase angle between plates
$\lambda$	wavelength of sinusoidal plates

especially for large values of the Reynolds number. A study of heat transfer in a channel composed of a smooth wall and a corrugated wall under conditions of laminar flow was made by [Fabbri \(2000\)](#). The heat transfer performance of the corrugated channel was compared with that of a channel made up of smooth walls. Their numerical model was coupled with a genetic algorithm program in order to optimize the corrugated plate profile in terms of heat transfer. On the other hand, [Fabbri and Rossi \(2005\)](#) conducted another study of heat transfer in the entrance region of a similar channel, comparing their results to the heat transfer coefficient in the entrance region of a flat plates channel; they analyzed the effect on the heat transfer of the Reynolds number and of the corrugated profile amplitude. [Zhang et al. \(2004\)](#), made a numerical study of the effects of the undulation and distance between plates on the convective heat transfer that presents in sinusoidal channels. Their results show that the heat transfer is enhanced for ratios distance between plates to wave amplitude larger than 0.5. [Niceno and Nobile \(2001\)](#), made a two-dimensional steady state numerical study of fluid flow and heat transfer in sinusoidal channels, and compared the heat transfer performance of sinusoidal and curved channels with that of a channel formed by flat walls. Their results indicate that the channel formed by arcs presents the largest heat transfer but it has greater pressure drop. [Gradeck et al. \(2005\)](#) studied experimentally the effects of hydrodynamics conditions on the enhancement of heat transfer for single phase flow. They found a local temperature distribution at the wall and its link with the local flow structure.

Several authors have analyzed in more detail the flow pattern and the conditions for the appearance of instabilities and chaoticity in the flow within sinusoidal channels: [Nishimura and Kawamura \(1995\)](#), studied the oscillatory flow in a two-dimensional symmetric sinusoidal wavy channel, and the important result that they obtained consists of the finding of a two-dimensional flow situation that becomes three-dimensional for a given value of the Strouhal number. [Lee et al. \(1999\)](#), made a numerical study of mass transfer in a wavy channel subject to a pulsating laminar flow. They obtained a chaotic behavior of the flow; this phenomenon of chaoticity showed a maximum for a certain Strouhal number, and this number was approximately equal to the inverse of the wavelength. [Stone and Vanka \(1999\)](#), studied the heat transfer in forced convection of a channel formed by 14 undulations. The geometric parameters were maintained constants and they made variations of the Reynolds number. Their results indicate that for small values of the Reynolds number,  $Re \leq 240$ , the channel shows total stability, characterized by recirculations in the upper and lower part. They found that the instability of the flow is accompanied by an increase in the heat transfer. An experimental study on the hydrodynamics and heat transfer of wavy channels was carried out by [Rush et al. \(1999\)](#). They studied the effects on flow and heat transfer of geometric parameters of the undulation and the Reynolds number. They classified the flow as steady and unsteady, and put special interest to determine the onset of macroscopic mixing and its influence on heat transfer. The onset of macroscopic mixing is found to depend on the channel geometry and the Reynolds number. Instabilities are reported to begin near the channel exit at low Reynolds and to move toward the channel entrance as the Rey-

nolds number is increased, with macroscopic mixing being present throughout the channel for moderate Reynolds numbers ( $Re \approx 800$ ). The authors reported the existence of a transversal velocity component when the flow becomes macroscopically mixed. [Kim \(2001\)](#) conducted an experimental study of developing and fully developed flows in a wavy channel, examining the onset position of the transition and the global mixing. [Mahmud et al. \(2002\)](#) carried out a numerical study analyzing the separation of the flow in channels formed by wavy surfaces, in which they varied the geometric parameters of the sinusoidal function. In their results they found a critical Reynolds number that marks the onset of separation. [Savino et al. \(2004\)](#) analyzed the pressure drop and heat transfer characteristics of a wavy channel that is nominally two dimensional, but used a three-dimensional numerical simulation for that. They found that the flow becomes three dimensional, not because of the action of boundary conditions, but due to the intrinsic fluid dynamical instabilities.

The present experimental investigation studies the flow pattern that appears in the entrance region of a channel formed by plates with sinusoidal corrugations. The types of instabilities as well as their relationship with the Reynolds number, the phase angle, and the spacing between corrugated plates is analyzed, presenting in this way a complete map of the ranges of appearance of the different flow features under laminar conditions.

## 2. Experimental apparatus and techniques

### 2.1. Flow visualization technique

The experiments were performed in a water tunnel with a test section 0.381 m wide, 0.508 m high and 1.5 m long. The walls and bottom of the test section are made of tempered glass for visual access to the model being tested. The water tunnel may be operated at velocities ranging from 0.01 to 0.3 m/s. The downstream end of the delivery plenum of the water tunnel has a section with flow conditioning elements. The first is a perforated stainless steel plate, which reduces the turbulence to a small scale, followed by a fiber-glass screen that further reduces the turbulence level. The last element is a honeycomb flow straightener. The contraction section of the water tunnel has an area ratio of 6:1. This geometry provides good velocity distribution, turbulence reduction and avoids local separation and vorticity development.

The experimental apparatus has a flowmeter from which the velocity of most of the cases is determined. These velocity estimations were verified by particle tracking at the core upstream of the model entrance. Pictures with a certain exposure time were taken to the traced particles; from where the velocity was obtained by dividing the captured length by the exposure time. It was found that the difference of the velocity deduced from the flowmeter and that obtained by the particle tracking technique described above was less than 3%.

The experimental velocity measurement uncertainty was determined by a procedure similar to that described by [Schraub et al. \(1965\)](#) for hydrogen bubble velocity measurements. The estimated uncertainty of the velocity calculation by particle tracking is 5.61%,

and is due mainly to uncertainties in the measurement of the displacement as a result of personal errors, optical distortion and image resolution.

Flow visualization experiments were achieved by seeding the water with  $14\text{ }\mu\text{m}$  diameter silver-coated hollow glass spheres. These glass spheres reflect the light emitted from a  $30\text{ mW}$  He-Ne laser tube that has been opened into a light sheet by use of a cylindrical lens. The laser light was cast through the bottom of the water tunnel to illuminate a fan-shaped plane that serves to keep track of the two-dimensional motion of the tracer particles on a vertical plane inside the experimental model. The room where the experiments took place was completely darkened in order to avoid the presence of any light source other than the laser light sheet.

A reflex photographic camera with a  $50\text{ mm}$   $f/2.5$  compact macro lens and a black and white photographic film were used to capture the streaks traced by the suspended particles. Exposure times were chosen depending on the flow velocity, and the values used were  $0.7$ ,  $1$ ,  $1.5$  and  $2\text{ s}$  with diaphragm adjustment of  $4.5$ ,  $5.6$  and  $6.7$ , respectively. Extended developing times were used in order to sensitize the negative to the presence of very dim light.

## 2.2. Design and construction of the experimental model

The experimental model was built by using a thermoforming technique to shape the  $2\text{ mm}$  thick Plexiglas plates to have a sinusoidal profile. The molds for the thermoforming of Plexiglas were made of aluminum plates  $25.4\text{ mm}$  thick, where the sinusoidal profile was carved by electro-erosion. The thermoforming process started by first heating the molds for  $15\text{ min}$  in an oven at  $300\text{ }^{\circ}\text{C}$ , followed by a heating of the Plexiglas plates in the same oven for

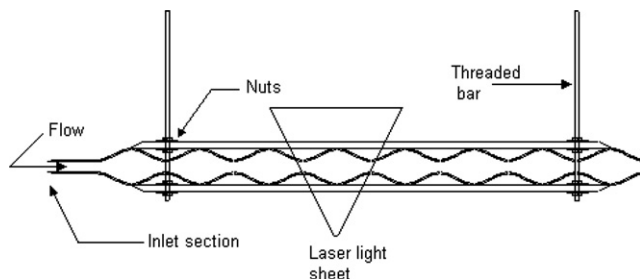


Fig. 1. Assembly of experimental model,  $\beta = 180^{\circ}$ .

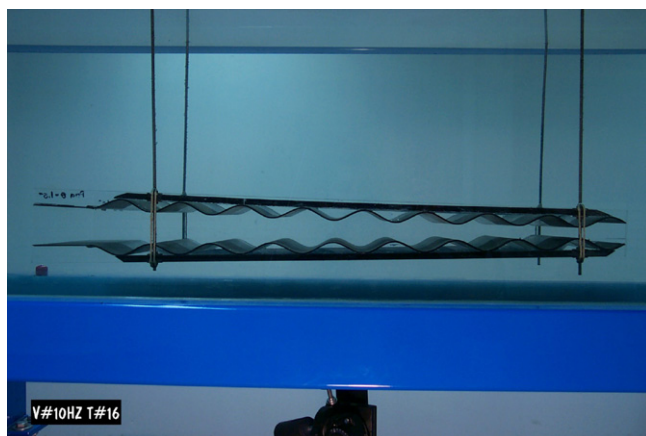


Fig. 2. Photograph of the experimental model.

$1.2\text{ min}$ . Once the Plexiglas was heated to the right temperature, it was pressed between the aluminum molds for about  $8$ – $10\text{ min}$  to impress in them the sinusoidal shape. The sinusoidal-shaped Plexiglas plates were cut and aligned to the size of the model and reinforced with  $25.4\text{ mm}$  wide,  $9\text{ mm}$  thick bars of the same acrylic to give the model rigidity. The bars were adhered to the plates by chloroform injection. The bars served also as support to the plates, the bars have a hole through which threaded rods support the model in each corner and through which the separation between plates is fixed. These threaded rods support the model to the frame of the water tunnel. A flat inlet section was added to the wavy channel in order to guarantee uniform horizontal flow at the inlet of the wavy channel. Sidewalls were added at each side of the wavy channel to make sure there is no leakage of the flow

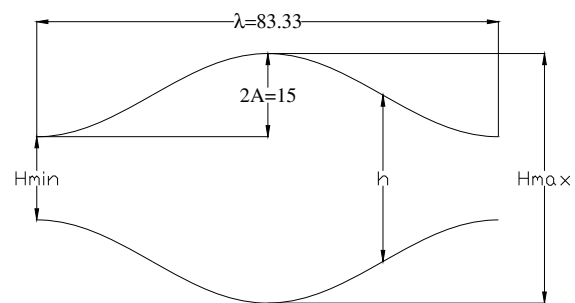


Fig. 3. Geometric parameters of a wave of the sinusoidal channel,  $\beta = 180^{\circ}$ .

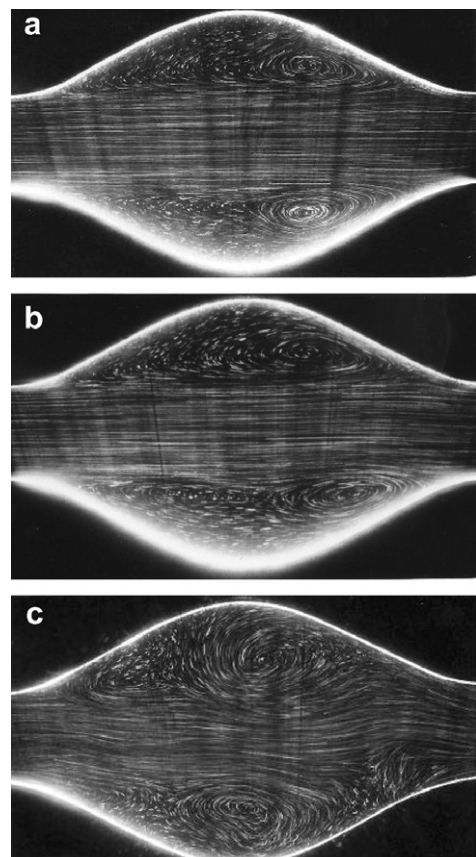
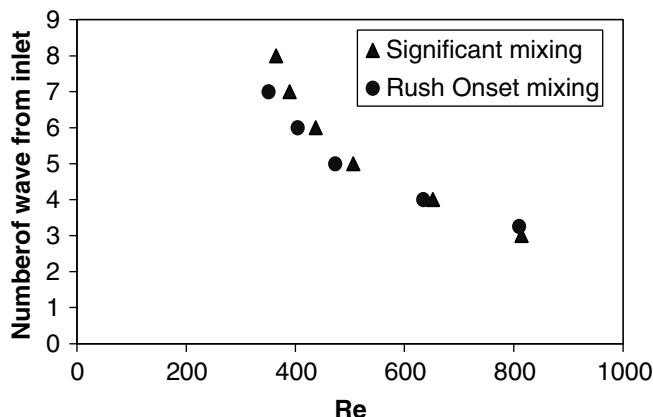


Fig. 4. Pictures of flow patterns that appear in a channel with  $\beta = 180^{\circ}$ ,  $\lambda/h = 2.77$  and  $A/h = 0.25$ . (a) Steady flow,  $Re = 470$ , second wave from inlet, (b) unsteady flow,  $Re = 470$ , fourth wave from inlet, (c) significantly-mixed flow,  $Re = 700$ , seventh wave from inlet.



**Fig. 5.** Validation of experimental results: (●) Results obtained by Rush et al. (1999), for  $\lambda/h = 2.77$ ,  $A/h = 0.24$  and  $\beta = 180^\circ$ . (▲) Results obtained in this investigation for  $\lambda/h = 2.77$ ,  $A/h = 0.25$  and  $\beta = 180^\circ$ .

through the sides of the channel. **Fig. 1** shows a schematic of the model assembly for  $\beta = 180^\circ$ . **Fig. 2** presents a picture of the model and how it is mounted in the experimental facility.

### 2.3. Experimental conditions

The experiments were performed in a wavy channel that contains eight waves having identical shape. **Fig. 3** shows the geometry and dimensions of a single wave of the channel for the case of a symmetrical channel ( $\beta = 180^\circ$ ). The average channel width,  $h$ , is kept constant for all waves by keeping parallelism between mid-plane lines of both plates, however the average channel width for the whole channel can be varied by adjusting the position of the upper plate. The phase angle between plates can also be modified by changing the upper plate by one that is longitudinally displaced.

The experimental study considered three different phase angles between the plates:  $\beta = 0$ ,  $\beta = 90$  and  $\beta = 180^\circ$ . Each one of these cases was studied for three different average distances between plates:  $h = 2.5$ ,  $h = 3.0$  and  $h = 3.5$  cm. The average channel width Reynolds number,  $Re = Vh/\nu$ , was varied from 200 to 1000. The flow behavior in every wave of the channel was analyzed in order to classify the flow. The flow conditions were determined and pictures were taken when graphical evidence of the flow features was required.

In a particular set of experiments, the effect of the number of waves in the channel on the hydrodynamics was studied. A channel with 12 waves was built, its flow features were determined,

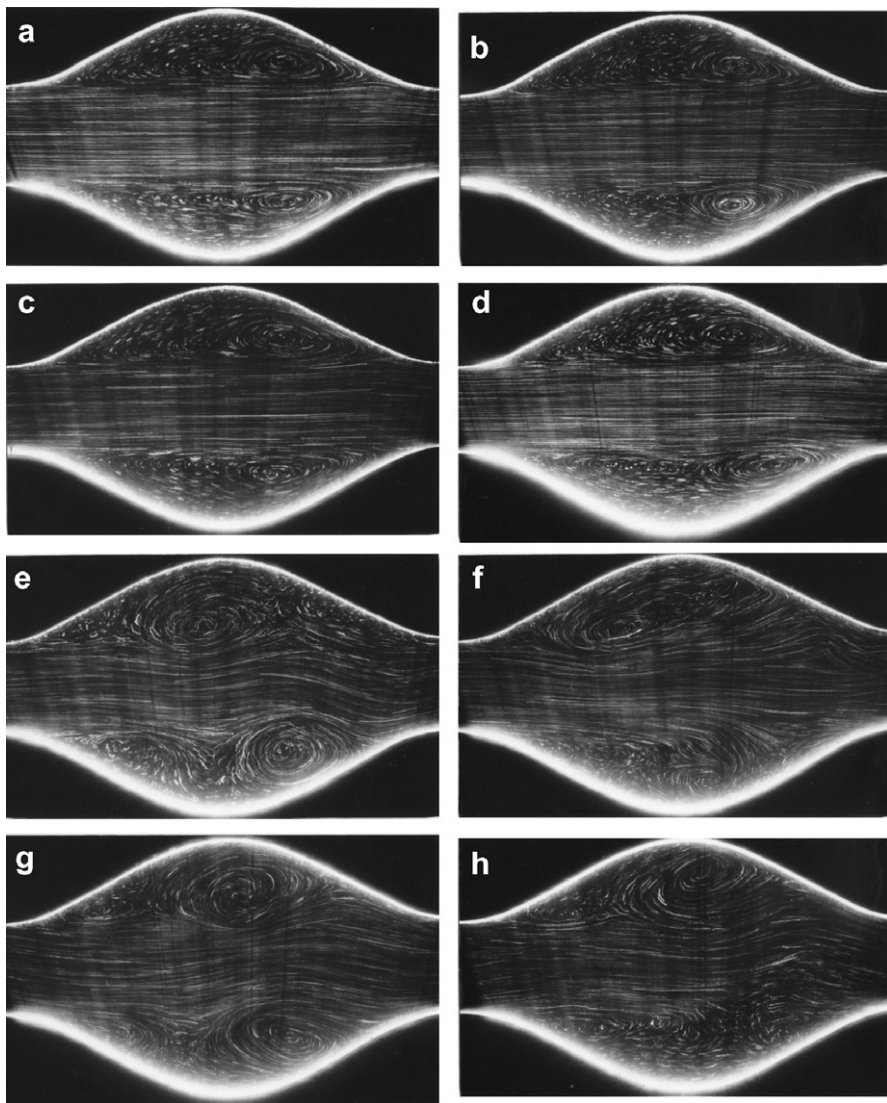


**Fig. 6.** Flow pattern along the channel, from the first wave (a) to the last wave (h).  $Re = 600$ ,  $\beta = 180^\circ$ ,  $\lambda/h = 2.77$  and  $A/h = 0.25$ .

and these were compared with those of a channel with eight waves.

### 3. Results and discussion

During the observations of the flow behavior for the configurations mentioned before, three types of flow conditions were found, which have been defined as steady, unsteady and significantly-mixed flows. Fig. 4 presents instantaneous pathlines showing clearly the difference between the flow features of the three classifications given above. In the steady flow behavior (Fig. 4a), recirculations with fixed positions appear in the upper and lower channel sections, the upper recirculation has a counterclockwise rotation and the lower recirculation has a clockwise rotation. If the plates are symmetrical with respect to the centerline of the channel, as in the case of  $\beta = 180^\circ$ , the flow is also symmetrical. The steady state flow appears mainly in the first waves from the inlet, it is lost relatively easily in the last waves, where the flow may become unsteady or significantly-mixed. The steadiness of the flow begins to give way to the other classifications of flow when the Reynolds number is increased or in further waves from inlet, presenting first small oscillations of the main flow, deformations in the recirculations, asymmetries in the flow and incipient exchange of fluid between the recirculations and the main flow. When any of these characteristics is present, it is said that the flow is unsteady, in this flow condition there are (especially when steadiness has just been lost) momentary asymmetries that last for a short period of time that become more evident and longer-lasting as the Reynolds number is increased (Fig. 4b). The significant-mixing flow condi-

tion (also called macroscopic mixing) appears later (for larger Reynolds numbers or further waves from inlet) than the unsteady flow, and is characterized by strong interactions between the main flow and the recirculations. Fig. 4c shows a picture of a flow presenting significant mixing. The significant-mixing flow is not symmetrical, even when the channel is symmetrical. The mixing of the main flow with the recirculations is present at all times and is time-dependent. In the region where significant mixing appeared, the flow turned into a 3-D phenomenon (Nishimura and Kawamura, 1995; Rush et al., 1999; Savino et al., 2004).

The experimental results obtained in this investigation for the case of parallel sinusoidal plates placed at  $\beta = 180^\circ$  were compared to the experimental results of Rush et al. (1999). These authors present a figure indicating the number of waves from inlet at which the flow becomes macroscopically mixed as a function of the Reynolds number. Fig. 5 shows curves indicating the number of waves from inlet,  $N$ , at which the flow presents macroscopic mixing for the cases of the work of Rush et al. (1999) and for the results obtained in this investigation. Fig. 5 then shows the good agreement between both investigations.

The progress of the flow along the entire channel is shown in Fig. 6. For the first waves the flow has clearly a steady behavior. As the fluid moves along the channel, it starts to show mixing between the upper and lower vortices and the main flow. The end of the channel shows more intensive mixing. It is concluded from this figure that the flow pattern goes from steady to unsteady, and from unsteady to significantly-mixed from inlet to outlet, regardless of the phase angle (that is, it is always observed for all cases that at the entrance region the flow is steadier than at the exit region, independently of the phase angle).

Fig. 7 shows the ranges at which each one of the flow classifications appear in a channel with  $\beta = 180^\circ$ , for two different average separations between plates. The appearance of the different flow regimes is a function of the Reynolds number and the number of wave from inlet. Fig. 7a shows results obtained for the case of  $\lambda/h = 2.77$  and  $A/h = 0.25$ ; in this case, as in all other cases, it was not possible to observe unsteady flows or significant mixing in the first wave from the inlet. The case  $\lambda/h = 2.38$  and  $A/h = 0.214$  appears in Fig. 7b, showing a slight displacement to larger Reynolds numbers of the appearance of the unsteady and significant-mixing flows.

The same classification of the flow described previously for the case  $\beta = 180^\circ$  applies to other cases, as in  $\beta = 90^\circ$ , with the differ-

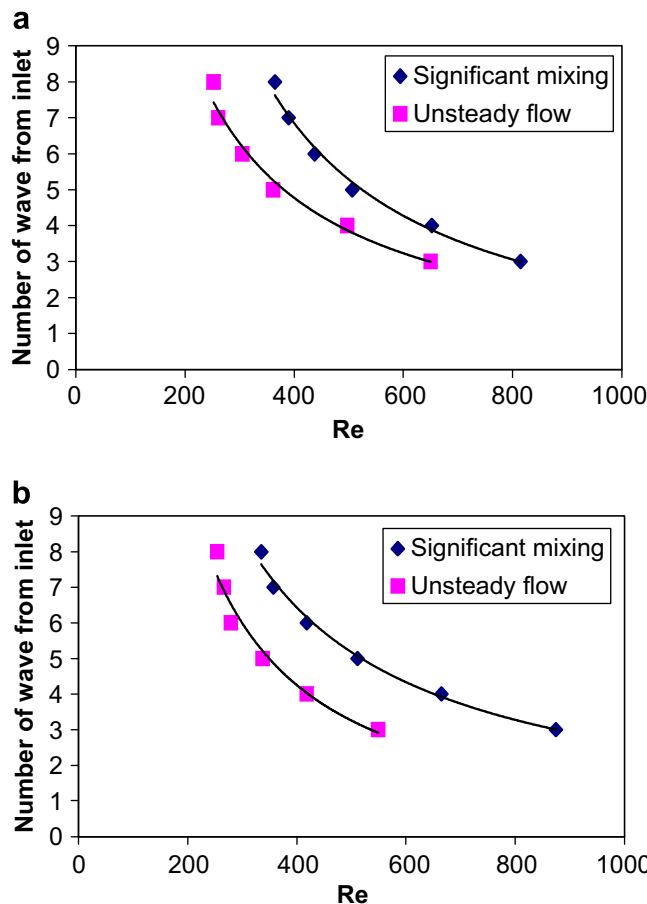


Fig. 7. Ranges of appearance of unsteady and significantly-mixed flow in channels with  $\beta = 180^\circ$ , (a)  $\lambda/h = 2.77$  and  $A/h = 0.25$ , (b)  $\lambda/h = 2.38$  and  $A/h = 0.214$ .

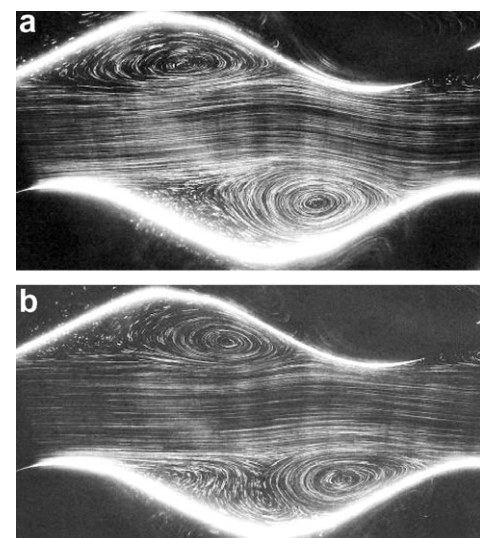


Fig. 8. Unsteady flow shown at two different times. Third wave from inlet,  $Re = 950$ ,  $\beta = 90^\circ$ ,  $\lambda/h = 3.33$  and  $A/h = 0.30$ .

ence here that the steady flow is not symmetrical because the channel is not symmetrical either. Fig. 8 shows the unsteady flow for a given set of flow and geometric parameters but at two different instants, here some characteristics of unsteady flows can be seen, such as slight vortex position displacements and variations in size without major interaction of vortices with the main flow (as in significantly-mixed flows). Fig. 9 shows the ranges at which each one of the flow classifications appear in a channel with  $\beta = 90^\circ$  for the two different average separations between plates. It can be seen that a decrease in the average channel width promotes unsteady flow appearing at lower Reynolds numbers, for the same wave number.

Fig. 10 shows two moments of the flow inside a  $\beta = 0^\circ$  channel for a given wave number from inlet and fixed  $Re$  and geometrical parameters. The flow that is shown in this set of pictures is significantly-mixed, as the main flow interacts with the recirculations in an intermittent way. The range of appearance of each one of the flow regimes in the case of  $\beta = 0^\circ$  shows a behavior similar to that of cases  $\beta = 90^\circ$  and  $\beta = 180^\circ$  that were presented before.

Fig. 11 compares the onset for appearance of significantly-mixed flows in channels with different  $\beta$  angles. Two different channel separations are presented in the figure. Fig. 11a, for the separation  $\lambda/h = 2.38$  and  $A/h = 0.214$ , shows that  $\beta = 180^\circ$  is the case where significant mixing appears first. In this case the channel configuration has a separation between plates that enables a better interaction between the core flow and the recirculations. Fig. 11b indicates that for smaller separations between plates, significant mixing appears first for  $\beta = 90^\circ$ .

The increase of the number of waves contained in the channel from 8 to 12 does not seem to have a significant influence on the

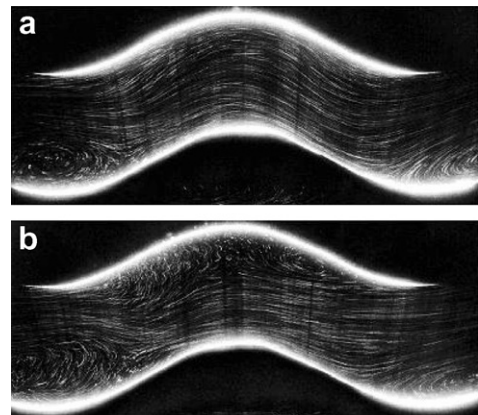


Fig. 10. Significantly-mixed flow in the 4th wave from inlet shown at two different instants.  $\beta = 0^\circ$ ,  $\lambda/h = 3.33$  and  $A/h = 0.30$ ,  $Re = 300$ .

appearance of the flow features in the channel. Fig. 12 shows the flow patterns of two channels with the same wave geometrical parameters and Reynolds number, one of the channels having 8 waves and the second 12 waves. The observations of Fig. 12 evidence that there is significantly-mixed flows in both cases for waves 5 and 6 from inlet. By analyzing the whole channel it was observed that the flow conditions on waves 1–8 are the same for both channels. This enables to affirm that, for the set of flow and geometric parameters used in the study, eight waves are enough to develop the flow in a channel of this class.

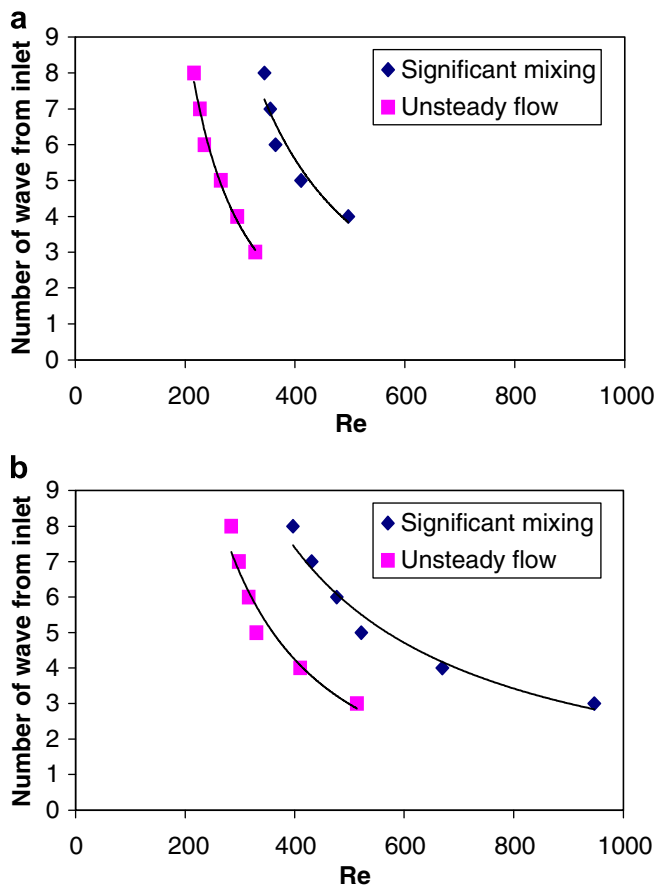


Fig. 9. Ranges of appearance of unsteady and significantly-mixed flow in channels with  $\beta = 90^\circ$ , (a)  $\lambda/h = 2.77$  and  $A/h = 0.25$ , (b)  $\lambda/h = 2.38$  and  $A/h = 0.214$ .

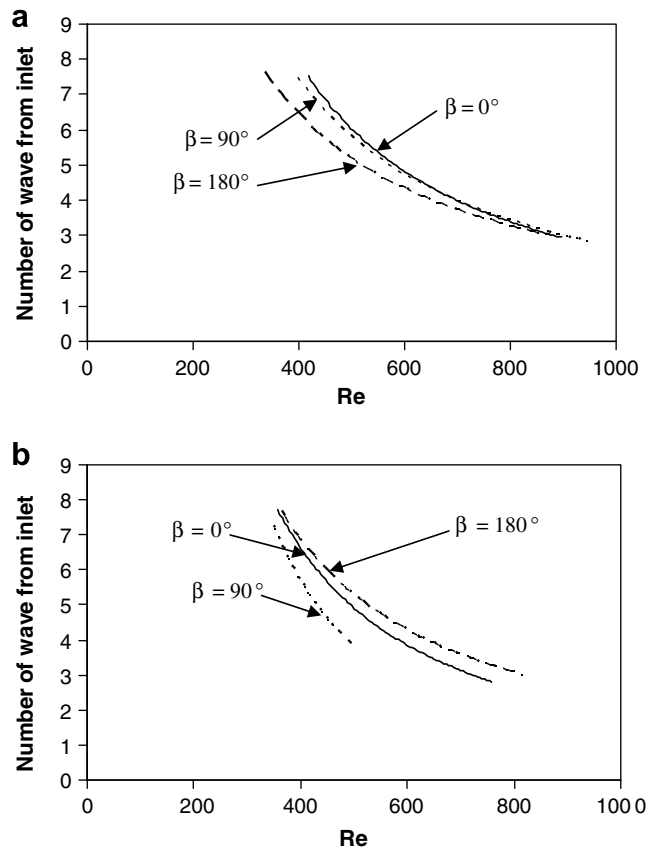
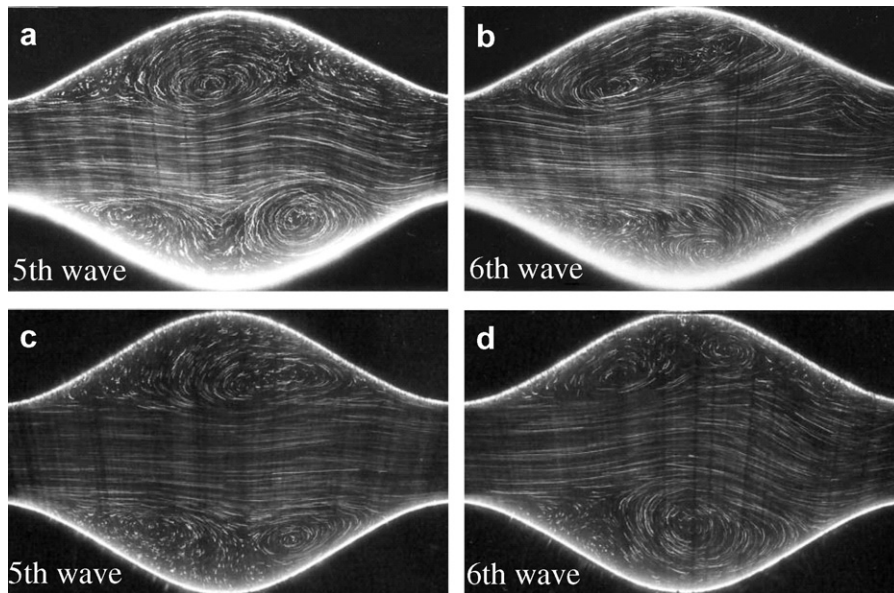


Fig. 11. Effect of the phase angle on the appearance of significantly-mixed flow regime: (a)  $\lambda/h = 2.38$  and  $A/h = 0.214$ , (b)  $\lambda/h = 2.77$  and  $A/h = 0.25$ .



**Fig. 12.** Similitude of flow patterns at the same wave of two channels with the same geometrical parameters, and different number of total waves. (a) and (b) are for an 8-waves channel, whereas (c) and (d) are for a 12-waves channel. For all cases  $\beta = 180^\circ$ ,  $\lambda/h = 2.77$ ,  $A/h = 0.25$ , and  $Re = 470$ .

#### 4. Conclusions

The flow regimes that were observed in this experiment are steady, unsteady and significantly-mixed flows. The instabilities of the flow appear in the end part of the channel and move towards the inlet of the channel as the Reynolds number is increased. For the range of Reynolds numbers tested, it was impossible to observe unsteady or significantly-mixed flows in the first wave from the inlet, and it was also difficult to find unsteady flows in the second wave from the inlet. For Reynolds numbers lower than 250 the channel presented steady flow along all of its length. The change of phase angle does not preclude the appearance of any of the flow regimes; but it modifies the Reynolds number at which the instabilities appear at a given wave from inlet; for small average channel width,  $\beta = 0^\circ$  is the case where significant mixing appears first, probably because the main flow is forced to follow the windings of the channel and interacts more with the recirculations. From the analysis of number of waves in a channel, it was demonstrated that, for the set of flow and geometric parameters used in the study, eight waves are enough to develop the flow in a channel of this class.

#### Acknowledgement

The authors would like to acknowledge the support of the Mexican Council for Science and Technology (CONACyT), under Grant J-37328-U. The authors also thank Mr. Manuel Lozano and Mr. Mauricio Azúa for their help and advice during the course of the experimental investigation.

#### References

Asako, Y., Faghri, M., 1987. Finite volume solutions for laminar flow and heat transfer in a corrugated duct. *Journal of Heat Transfer* 109, 627–634.

Fabbri, G., 2000. Heat transfer optimization in corrugated wall channels. *International Journal of Heat and Mass Transfer* 43, 4299–4310.

Fabbri, G., Rossi, R., 2005. Analysis of the heat transfer in the entrance region of optimised corrugated wall channel. *International Communications in Heat and Mass Transfer* 32, 902–912.

Gradeck, M., Hoareau, B., Lebouché, M., 2005. Local analysis of heat transfer inside corrugated channel. *International Journal of Heat and Mass Transfer* 48, 1909–1915.

Gschwind, P., Regele, A., Kottke, V., 1995. Sinusoidal wavy channels with Taylor-Görtler vortices. *Experimental Thermal and Fluid Science* 11, 270–275.

Kim, S.K., 2001. An experimental study of developing and fully developed flows in a wavy channel by PIV. *KSME International Journal* 15, 1853–1859.

Lee, B.S., Kang, I.S., Lim, H.C., 1999. Chaotic mixing and mass transfer enhancement by pulsatile laminar in an axisymmetric wavy channel. *International Journal of Heat and Mass Transfer* 42, 2571–2581.

Mahmud, S., Islam, S.A.K.M., Mamun, M.A.H., 2002. Separation characteristics of fluid flow inside two parallel plates with wavy surface. *International Journal of Engineering Science* 40, 1495–1509.

Niceno, B., Nobile, E., 2001. Numerical analysis of fluid flow and heat transfer in periodic wavy channels. *International Journal of Heat and Fluid Flow* 22, 156–167.

Nishimura, T., Kawamura, Y., 1995. Three-dimensionality of a oscillatory flow in a two-dimensional symmetric sinusoidal wavy-walled channel. *Experimental Thermal and Fluid Science* 10, 62–73.

Rush, T.A., Newell, T.A., Jacobi, A.M., 1999. An experimental study of flow and heat transfer in sinusoidal wavy passages. *International Journal of Heat and Mass Transfer* 42, 1541–1553.

Savino, S., Comini, G., Nonino, C., 2004. Three-dimensional analysis of convection in two-dimensional wavy channels. *Numerical Heat Transfer Part A – Applications* 46, 869–890.

Schraub, F.A., Kline, S.J., Henry, J., Rustlander, P.W., Litell, A., 1965. Use of hydrogen bubbles for quantitative determination of time-dependent velocity fields in low-speed water flows. *Journal of Basic Engineering* 87, 429–444.

Stone, K., Vanka, S.P., 1999. Numerical study of developing flow and heat transfer in a wavy passage. *Journal of Fluids Engineering* 121, 713–719.

Tsal, S.F., Sheu, T.H.W., Lee, S.M., Mitra, N.K., 1999. Heat transfer in a conjugate heat exchanger with a wavy fin surface. *International Journal of Heat and Mass Transfer* 42, 1735–1745.

Vasudeviah, M., Balamurugan, K., 2001. On forced convective heat transfer for a Stokes flow in a wavy channel. *International Communications in Heat and Mass Transfer* 28, 289–297.

Wang, C.-C., Chen, C.-K., 2002. Forced convection in a wavy-wall channel. *International Journal of Heat and Mass Transfer* 45, 2587–2595.

Wang, C.C., Jang, J.Y., Chiou, N.F., 1999. A heat transfer and friction correlation for wavy fin-and-tube heat exchangers. *International Journal of Heat and Mass Transfer* 42, 1919–1924.

Zhang, J., Kundu, J., Manglik, R.M., 2004. Effect of fin wavy and spacing on the lateral vortex structure and laminar heat transfer in wavy-plate-fin cores. *International Journal of Heat and Mass Transfer* 47, 1719–1730.